# Accuracy Issues in a High-Level Model for MEMS Varactors

Janakiram G. Sankaranarayanan, Manas Behera
School of Electrical Engineering & Computer Science
Oregon State University
Corvallis, OR-97331, USA
sankaraj@ece.orst.edu, behera@ece.orst.edu

Narayan Aluru
Beckman Institute for Advanced Science and Technology
University of Illinois at Urbana-Champaign
Urbana, IL-61801, USA
aluru@uiuc.edu

Kartikeya Mayaram
School of Electrical Engineering Computer Science
Oregon State University
Corvallis, OR-97331,USA
karti@ece.orst.edu

**Abstract**

This paper presents accuracy issues for an equivalent circuit model and an AHDL model (high-level models) of MEMS varactors. Simulations of different MEMS varactor structures were done using the high-level models and an electrostatic/mechanical solver EM8.9. The limitations of the varactor high-level models are presented in the context of a RF MEMS VCO operating at 1.6 GHz in a TSMC 0.35 μm CMOS technology.

Keywords- High-level model, MEMS varactors, electrostatic/mechanical solver, RF MEMS VCO

## I Introduction

Recent developments in micromachining technology have made possible the implementation of MEMS-based varactors. Compared with solid-state varactors, MEMS-based varactors have the advantages of lower loss and potentially greater tuning range. In addition to having a high Q factor and a wide tuning range, these devices can also withstand large voltage swings, thus making them suitable for low phase noise VCO applications [1].

The design of a MEMS VCO requires the combination of the MEMS varactors with conventional integrated circuit technology. Such mixed-technologies can lead to highly efficient, low cost systems with a wide range of applications. A crucial part in the design phase of such mixed-technology systems is the verification of their behavior by simulation. Therefore, accurate macromodels for the MEMS varactors are necessary in simulating the performance of RF MEMS VCOs.

In this paper, we compare two different methods for modeling the MEMS varactor structures. An equivalent circuit model [2] and a behavioral model are compared with numerical simulations from an electrostatic/mechanical solver EM8.9 [3]. Accuracy issues of the high-level models are identified in the context of RF MEMS VCOs. The equivalent circuit model and the behavioral model are described in Section II and a brief description of the electrostatic/mechanical solver EM8.9 is provided in Section III. The different MEMS varactor structures are described in Section IV. Simulation results of these MEMS varactor structures and the effects of different materials and different dimensions on their tuning characteristics are illustrated in Section V. Comparisons between the simulation results obtained from the high-level model and the electrostatic/mechanical solver are discussed and conclusions are drawn in Section VI.

This work is supported in part by NSF grant CCR – 0121616.

## II High-Level Model for MEMS Capacitor

*A. Working Principle*

The functional model of an electro-mechanically tunable capacitor shown in Fig. 1 consists of two parallel plates. The top plate of the capacitor is suspended by a spring with spring constant *k*, while the bottom plate of the capacitor is fixed. When a bias voltage is applied across the capacitor plates, the suspended plate is attracted towards the bottom plate due to the resultant electrostatic force. The suspended plate moves towards the fixed plate until equilibrium between the electrostatic and the spring forces is reached.

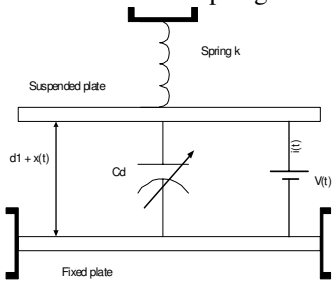


Fig. 1. Functional model of an electro-mechanically tunable parallel-plate capacitor with two parallel plates.

At equilibrium, the electrostatic force and the spring force can be equated as given below [2]

$$kx = - \epsilon_0 A V^2 / 2(d_1 + x)^2 \quad (1)$$

where, $\epsilon_0$ = 8.85415 x $10^{-12}$ F/m,
$A$ = area of the capacitor plates,
$d_1$ = separation of the capacitor plates for no applied bias voltage,
$x$ = displacement of the suspended plate,
$k$ = spring constant,

$V$ = applied voltage.

The parallel plate capacitance $C_d$ is given by [2]

$$C_d(V) = \epsilon_0 A / (d_1 + x\,(V)) \qquad (2)$$

It should be noted that the suspended plate will make contact with the bottom plate if the electrostatic force is greater than the spring force, which occurs when $x < d_1/3$. Therefore, the maximum theoretical tuning range is 1.5:1 [2].

*B. Mechanical Characteristics*

The MEMS capacitor can be modeled as a mass-spring-damper systems as shown in Fig. 2. There are two parallel plates, the top one is restrained by a spring and damper and the bottom plate is fixed. The spring represents the restoring force from the support of the top plate, while the damper represents the air resistance. With no applied bias the weight and the spring force on the top plate reach equilibrium. The damper has an effect only when the plate is in motion [4]. The dynamics of the electro-mechanical system can be described as follows

$$m\,d^2x/dt^2 + r\,dx/dt + k\,x = -\,\epsilon_0 A V^2 / 2(d_1 + x)^2 \qquad (3)$$

where, $m$ = mass of the suspended plate
$r$ = mechanical resistance

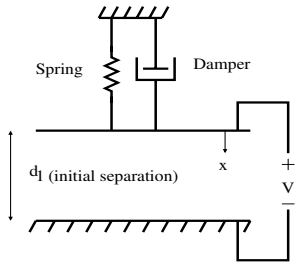


Fig. 2. Mass-spring-damper model of the MEMS capacitor.

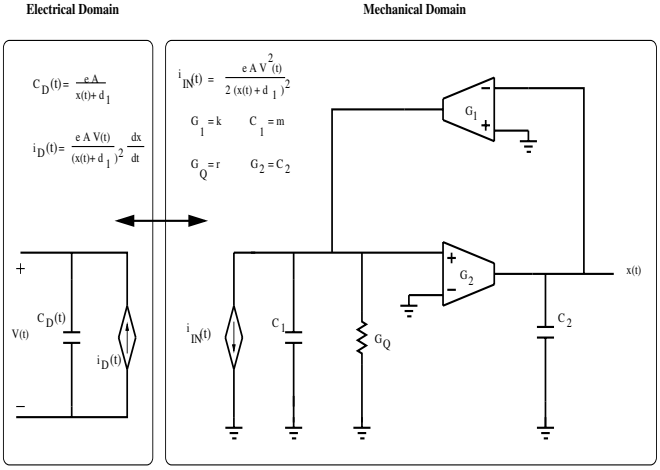


Fig. 3. Equivalent circuit model of an electro-mechanically tunable capacitor.

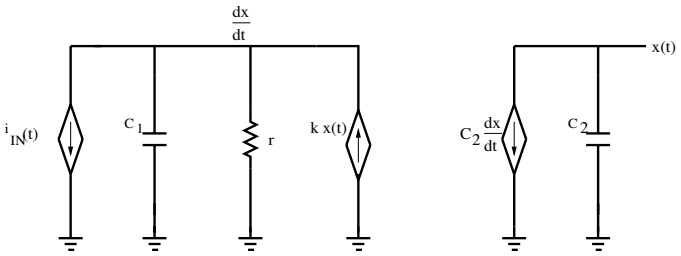


Fig. 4. Equivalent circuit model of an electro-mechanically tunable capacitor for implementation in HSPICE.

*C. Equivalent Circuit Model*

The equivalent circuit model as presented in [2] for a tunable capacitor with two parallel plates is shown in Fig. 3. This circuit model is based on Eq. (1).The right-hand side term $\epsilon_0 A V^2 / 2(d_1 + x)^2$ of Eq. (3) represents the electrostatic driving force and is modeled as a current source $i_{IN}(t)$ in the equivalent circuit of Fig.3. The mass, $m$, of the suspended plate is modeled as an equivalent capacitor while the mechanical resistance is modeled as a resistor. The spring constant $k$ is represented as an equivalent transconductance $G_1$ and the transconductor $G_2$ and capacitor $C_2$ are used as an integrator.

The corresponding equivalent circuit model that was implemented in HSPICE for simulation is shown in Fig. 4. The transconductors $G_1$ and $G_2$ have been modeled as ideal voltage controlled current sources.

*D. Behavioral Model*

The behavior of the MEMS capacitor can be completely described using Eq. (3). Based on this equation a behavioral model was developed and implemented in SpectreHDL. Simulated results of this model show exact agreement with the equivalent circuit model.

## III The Electrostatic/Mechanical Solver

EM8.9 is a simulator for electrostatic MEMS analysis and can accurately simulate the characteristics of MEMS varactors. EM 8.9 employs the finite cloud method (FCM) for mechanical analysis and the boundary cloud method (BCM) for electrostatic analysis. FCM and BCM methods obviate the need for complicated and time consuming mesh generation [3]. Lagrangian descriptions are used to map the electrostatic analysis to the undeformed geometry of conductors, thus eliminating the need for geometry updates and re-computation of the interpolation functions [3]. The procedure for the self- consistent analysis of coupled electromechanical devices can be summarized as follows [3]. Electrostatic analysis using BCM is done first to compute the surface charge density and the electrostatic pressure, which is then used in the mechanical analysis (performed on the undeformed geometry by FCM) to compute the structural displacement. The geometry is then updated and the capacitance is computed. This procedure is repeated until a state of equilibrium is achieved.

## IV MEMS Capacitor Structures

Different MEMS capacitor structures were simulated using the high-level models and the simulator EM8.9 and their tuning characteristics were compared. An overlap area of 230 µm x 230 µm and an air gap of 0.75 µm were used for all the structures which results in a nominal capacitance of 0.624 pF.

### *A. Cantilever Beams and Fixed-Fixed Beams*

Cantilever beams and fixed-fixed beams are the simplest forms of electro-statically actuated MEMS-based capacitor structures. These structures and their deformation due to the application of an external bias voltage are shown in Figs. 5 (a) and (b). The working principle of these capacitors are based on Eq. (1) where, the stiffness constant, $k$, for the cantilever beam capacitor and the fixed-fixed beam capacitor depend on the dimensions of the capacitor itself and are expressed as given in (4) and (5), respectively [4].

$$k_{cant}=2/3EW(t/L)^3 \quad (4)$$

and, $$k_{fixed}=32E\,W\,(t/L)^3 \quad (5)$$

where, $E$ is the Young's modulus of the material of the capacitor, and $W$, $t$, $L$ are the width, thickness, and length of the suspended plate, respectively.

### *B. Parallel Plate Capacitor with Suspension Structures*

The top view of a MEMS based capacitor with suspension structures is shown in Figs. 6 (a) and (b). The suspension structures are designed to obtain the stiffness constant and thus the desired tuning range. The stiffness constant of a suspension structure with length $L$, width $W$ and thickness $t$ is given by [2], [4].

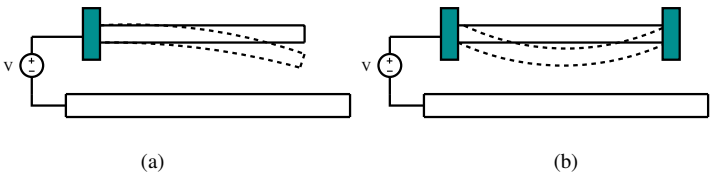


Fig. 5. (a) Cantilever beam and (b) fixed-fixed beam capacitor.

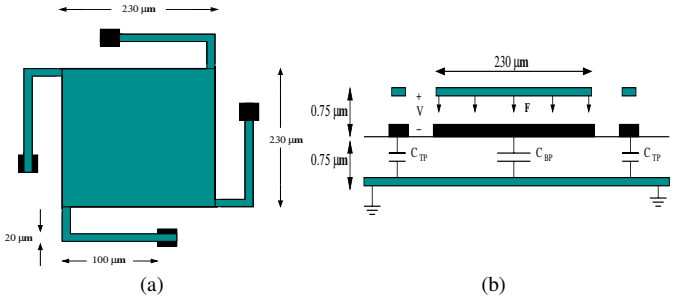


Fig. 6. (a) Top view and (b) cross-sectional view of the parallel plate capacitor

$$k=EW(t/L)^3 \quad (6)$$

From Eq. (6) it can be seen that the spring constant is linearly proportional to the beam width and highly dependent on beam length and thickness. Therefore by varying the dimension of the suspension structures, different beam stiffnesses can be obtained for various tuning voltages. The simulated structure had an equivalent spring constant of 44 N/m with a tuning voltage of 3.3 V. The length and width of the suspension structure were chosen as 100 µm and 20 µm, respectively.

## V Results

Simulations were performed for the parallel plate capacitor, cantilever beam capacitor and fixed-fixed beam capacitor using the high-level models and the numerical solver EM8.9. The comparisons between the results obtained for the AHDL model and the numerical solver have been illustrated below.

As mentioned earlier the stiffness constant of the MEMS varactor is an important design parameter since it determines the tuning ratio of the varactor. Fig. 7 shows the capacitance as a function of the stiffness constant for different applied voltages. For the parallel plate capacitor the tuning ratio is determined by the stiffness constant of the suspension structure given by Eq. (6) assuming the capacitor plate is rigid [2]. However, the non-rigid nature of the suspended plate also contributes to the overall stiffness constant of the MEMS structure. The stiffness constant of the suspended plate depends on its dimensions. Since the length and width (area) of the suspended plate is fixed by the desired capacitance, simulations were done for different thicknesses of the suspended plate. Fig. 8 shows the capacitance as a function of voltage for different thicknesses of the parallel plate capacitor as simulated by EM8.9. It can be observed that the capacitance tuning characteristic is affected with varying thickness. The increase in the tuning voltage with increasing thickness can be accounted for by the fact that the stiffness constant of the top plate and hence the overall stiffness constant increases with thickness.

The high-level models fail to account for the thickness of the top plate and therefore its stiffness constant. This reflects as a discrepancy between the C-V curves obtained from the model and the EM8.9 simulator as shown in Fig. 9. Simulations performed by using the high-level models show a capacitance tuning ratio of 1.45 for a tuning voltage of 3.42 V, whereas, the simulated results from EM8.9 show a capacitance tuning ratio of 1.43 for a tuning voltage of 3.3 V with an error of 3.6 %.

Another drawback of the high-level models is that they are incapable of simulating MEMS capacitor structures

such as the cantilever and fixed-fixed beam capacitors. In the parallel plate capacitor with suspension structures the displacement caused by the electrostatic force is uniform along the length of the suspended plate. For fixed-fixed beam and cantilever beam capacitors, the displacement of the top plate varies along its length, being maximum at the center for the fixed-fixed beam and at the free end for the cantilever beam. Simulated results obtained from EM8.9 show the structural displacement along the length of the suspended plate in Figs. 10 (a) and (b). Since the high-level models do not account for the change in displacement along the length of the suspended plate, the C-V curves of the cantilever and fixed-fixed beam capacitors as illustrated in Figs. 11 (a) and (b), respectively, deviate significantly from EM8.9.

The parallel plate MEMS capacitor structure was simulated for three different materials, polysilicon/gold, aluminum, and nickel/gold. The tuning characteristics obtained from the model and EM8.9 show similar trends as shown in Fig. 12. However, an error exists between the C-V curves due to reasons discussed earlier.

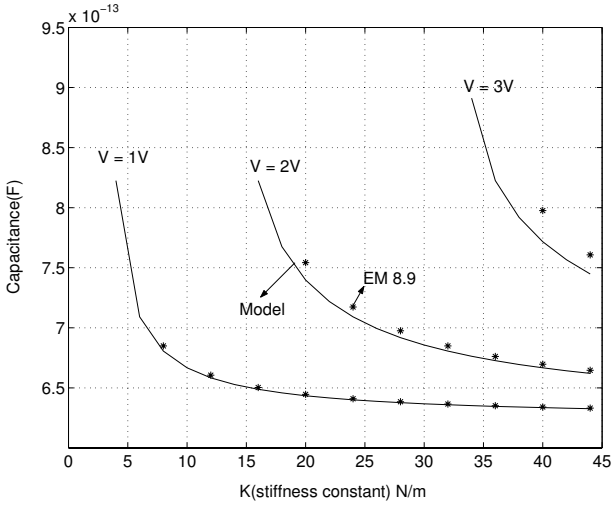


Fig. 7. Capacitance as a function of the stiffness constant.

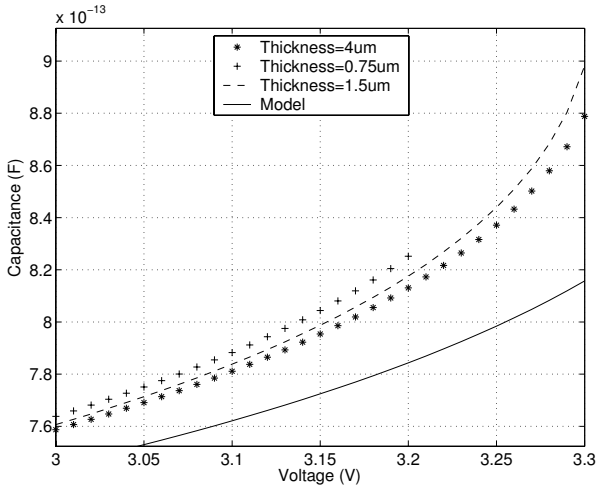


Fig. 8. Capacitance as a function of voltage for varying thicknesses of the suspended plate.

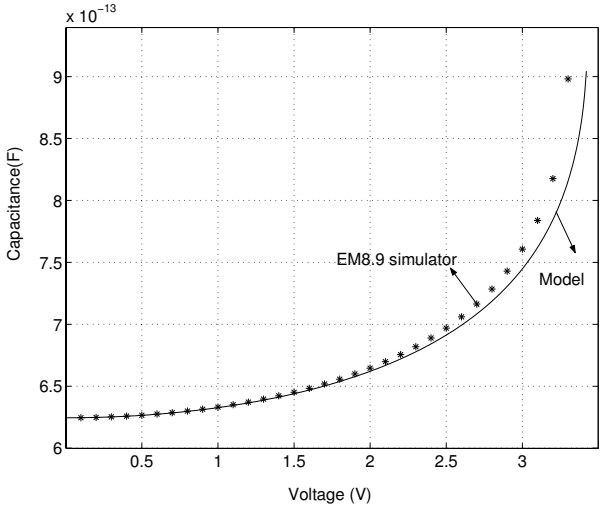


Fig. 9. Capacitance versus voltage characteristics for the parallel plate MEMS capacitor with suspension structures.

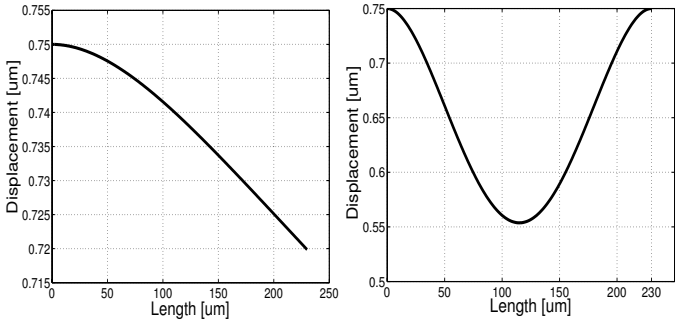


(a) (b)

Fig. 10. Structural displacement along the length of (a) cantilever beam, (b) fixed-fixed beam.

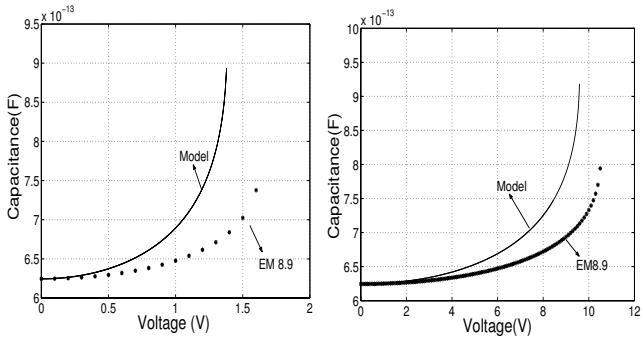


(a) (b)

Fig. 11. Capacitance versus voltage characteristics for (a) cantilever beam capacitor, and (b) fixed-fixed beam capacitor.

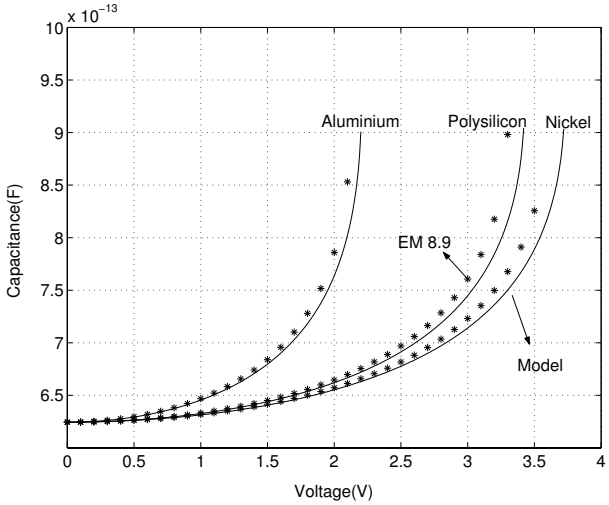


Fig. 12. Capacitance versus voltage characteristics for different materials.

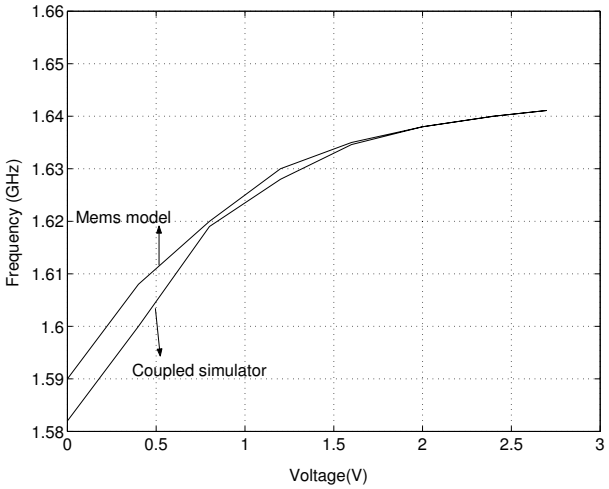


Fig. 14. VCO tuning characteristics.

*VCO simulations*

A 1.6 GHz VCO [5] implemented in a TSMC 0.35µm CMOS technology was simulated. The schematic of the VCO circuit is as shown in Fig. 13. The circuit was simulated using the AHDL model in SpectreS and the coupled circuit/device simulator (SPICE3f5/EM8.9) [6]. The frequency tuning characteristics of this VCO are shown in Fig. 14. The VCO simulated with the AHDL model show a tuning range of 1590 MHz to 1640 MHz with a tuning voltage of 2.7 V, whereas, coupled simulations show a tuning range of 1580 MHz to 1640 MHz with the same tuning voltage. The amplitude of oscillation was 2.5 V. The differences in the curves are consistent with differences observed in the corresponding C-V curves. It was also observed that both the AHDL model and the coupled simulator resulted in the same amplitude of oscillation.

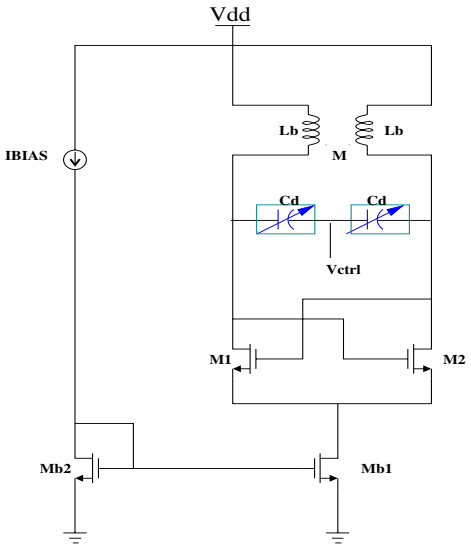


Fig. 13. Schematic of the VCO circuit.

## VI Conclusion

Comparisons between the high-level models and a numerical device solver have been presented for the simulations of MEMS based varactors. Issues related to the accuracy of the high-level models have been identified. The high-level models do not account for the stiffness constant of the non-rigid suspended plate and, therefore, an error exists in the C-V curves for higher control voltages. Simulations performed for three different materials also show similar trends. For lower voltages, the high-level models are accurate and can be used for the simulation of RF MEMS VCOs.

## References

[1] D. Young and B. E. Boser, "A micromachined –based RF low noise voltage controlled oscillator," in *IEEE Proc. CICC*, May 1997, pp. 431-434.

[2] A. Dec and K. Suyama, "Micromachined electro-mechanically tunable capacitors and their application to RF ICs," *IEEE Trans. Microwave Theory Tech.*, vol. 46, pp. 2587-2595, Dec 1998

[3] G. Li and N. R. Aluru, "Efficient mixed-domain analysis of electrostatic MEMS*," IEEE/ACM Digest of Technical papers, International Conference on Computer-Aided Design*, pp. 474-477, San Jose, Nov.10-14, 2004.

[4] Gabriel M. Rebeiz, *RF MEMS Theory, Design and Technology,* John Wiley & Sons, 2003.

[5] A. Dec and K. Suyama, "Microwave MEMS-based voltage controlled oscillators," *IEEE Trans. Microwave Theory Tech.*, vol. 48, pp. 1943-1949, Nov. 2000.

[6] M. Behera, S. De, N. Aluru and K. Mayaram, "A Coupled Circuit and Device Simulator for Design of RF MEMS VCOs," in *IEEE-Nano Conf.*, San Francisco, Aug. 12-14, 2003.